HHS Public Access

Author manuscript

Glia. Author manuscript; available in PMC 2021 May 01.

Published in final edited form as:

Glia. 2021 May ; 69(5): 1155–1169. doi:10.1002/glia.23955.

The complement C3-C3aR pathway mediates microglia-astrocyte interaction following status epilepticus

Yujia Wei[1,2], **Tingjun Chen**[1], **Dale B. Bosco**[1], **Manling Xie**[1], **Jiaying Zheng**[1], **Aastha Dheer**[1], **Yanlu Ying**[1], **Qian Wu**[1], **Vanda A. Lennon**[1,3], **Long-Jun Wu**[1,3,4,*]

[1]Department of Neurology, Mayo Clinic, Rochester, MN, 55905, USA

[2]Department of Neurosurgery, Xinqiao Hospital, Army Military Medical University, Chongqing, 400037, China

[3]Department of Immunology, Mayo Clinic, Rochester, MN, 55905, USA

[4]Department of Neuroscience, Mayo Clinic, Jacksonville, FL, 32224, USA

Abstract

Gliosis is a histopathologic characteristic of epilepsy that comprises activated microglia and astrocytes. It is unclear whether or how crosstalk occurs between microglia and astrocytes in the evolution of epilepsy. Here, we report in a mouse model of status epilepticus, induced by intracerebroventricular injection of kainic acid (KA), sequential activation of microglia and astrocytes and their close spatial interaction in the hippocampal CA3 region. Microglial ablation reduced astrocyte activation and their upregulation of complement C3. When compared to wild-type mice, both $C3^{-/-}$ and $C3aR^{-/-}$ mice had significantly less microglia-astrocyte interaction in response to KA-induced status epilepticus. Additionally, KA-injected $C3^{-/-}$ mice had significantly less histochemical evidence of neurodegeneration. The results suggest that the C3-C3aR pathway contributes to KA-induced neurodegeneration by mediating microglia-astrocyte communication. The C3-C3aR pathway may prove to be a potential therapeutic target for epilepsy treatment.

Keywords

Complement C3; C3a receptor; epilepsy; seizures; gliosis; microglia; astrocytes; kainic acid

1 | INTRODUCTION

Epilepsy is a common neurological disorder affecting approximately 70 million people worldwide. Most therapies are based on neurocentric mechanisms to which at least one-third of patients become refractory. Alternative and complementary therapeutics are sought (Thijs, Surges, O'Brien, & Sander, 2019). Increasing evidence assigns glial cells a role in epilepsy

[*]**CORRESPONDENCE:** ***Dr. Long-Jun Wu***, Department of Neurology, Mayo Clinic, 200 First Street SW, Rochester, MN 55905, Phone: (617) 943-7822, wu.longjun@mayo.edu.

Conflict of Interest: The authors declare no competing financial interests.

DATA AVAILABILITY STATEMENT

The data of this study are available from the corresponding author upon reasonable request.

pathogenesis. Targeting those cells could complement existing treatment strategies. Extensive activation of microglia and astrocytes is observed in animal models of epilepsy and in cerebral tissues resected from epileptic patients (Eyo, Murugan, & Wu, 2017; Feng et al., 2019; Patel, Tewari, Chaunsali, & Sontheimer, 2019; Shapiro, Wang, & Ribak, 2008). Gliosis results from activation of microglia and astrocytes in response to CNS damage and ultimately leads to glial scar formation (Bedner et al., 2015; Deshpande et al., 2020; Sofroniew & Vinters, 2010; Szalay et al., 2016). Gliosis can be beneficial, by helping maintain the extracellular environment and restoring blood-brain barrier function, or detrimental by increasing regional concentrations of neurotoxic inflammatory substances, impairing functional recovery, and worsening clinical signs (Sofroniew, 2009; D. Zhang, Hu, Qian, O'Callaghan, & Hong, 2010). Epilepsy acquired from traumatic brain injury or stroke is thought to be partially caused by gliosis, because surgical removal of glial scars in patients with drug-resistant epilepsies can alleviate seizures (Robel, 2017; Robel et al., 2015). It is unclear whether microglia-astrocyte crosstalk occurs in the course of gliosis and subsequent epileptogenesis.

Certain complement components of the innate immune system play important roles in several neurological disorders (Chavan, Pavlov, & Tracey, 2017; Kipnis, 2016). This pathway is activated when the recognition complement protein C1q binds to the cell surface, inducing C3 convertase activation and subsequent proteolytic cleavage of C3 into C3a and C3b fragments (Barnum, 2017; Wagner & Frank, 2010). Studies have shown that RNA transcripts and protein levels of C1q and C3 are increased in the hippocampus of patients with temporal lobe epilepsy (TLE) (Aronica et al., 2007; Schartz, Wyatt-Johnson, Price, Colin, & Brewster, 2018; Wyatt, Witt, Barbaro, Cohen-Gadol, & Brewster, 2017). Furthermore, long-lasting complement C1q-C3 signaling activation in status epilepticus correlates with epileptic seizure frequency (Schartz et al., 2018). C1q can induce astrocytes to change to A1 neurotoxic phenotype (Liddelow et al., 2017), and when status epilepticus is induced in C1q-null mice, they exhibit enhanced synaptic connectivity and remodeled dendritic spines (Chu et al., 2010). In the CNS, C1q is principally produced by microglia and C3 by activated astrocytes (Lian et al., 2015; Y. Zhang et al., 2014). Furthermore, the receptor for the C3a fragment of C3 (C3aR) is mainly expressed by activated microglia (Davoust, Jones, Stahel, Ames, & Barnum, 1999; Y. Zhang et al., 2014). Recent studies show that C3-C3aR signaling involves in several lesion-related neuronal damage. This signaling pathway mediates tau pathogenesis via STAT3 in Alzheimer's disease (Litvinchuk et al., 2018) and also drives involving neuromyelitis Optica (NMO) lesion(Chen et al., 2020). Consequently, we hypothesized involvement of complement-mediated crosstalk between microglia and astrocytes in the gliosis reaction related to epilepsy. The objectives of this study were: (1) to investigate spatial and temporal aspects of the complement C3-C3aR pathway as a potential mediator of microglia-astrocyte interaction; and (2) to determine whether glial activation via C3-C3aR signaling occurs in the course of neurodegeneration following KA-induced status epilepticus. This study points to C3 signaling as a novel therapeutic target to inhibit gliosis and hippocampal neurodegeneration under epileptic conditions.

2 | METHODS

2.1 | Animals

All procedures were approved by the Mayo Clinic Institutional Animal Care and Use Committee (IACUC) and accorded with institutional guidelines. All experiments used male mice, aged 6–8 weeks. Wild-type C57BL/6J (WT) mice were purchased from Charles River Laboratories, $C3^{-/-}$ mice (B6;129S4-$C3^{tm1Crr/J}$) and $C3aR^{-/-}$ mice (C.129S4-$C3ar1^{tm1Cge/J}$) were purchased from Jackson Laboratories (Bar Harbor, ME). Mice were housed in standard caging and maintained under controlled temperature and humidity, with 12/12-h light/dark cycles.

2.2 | Status epilepticus induction and seizure quantification:

Status epilepticus was induced by injecting kainic acid (KA) as described previously (Eyo et al., 2015; Eyo et al., 2014), by implanting a 26-gauge stainless steel guide cannula aimed towards the lateral cerebral ventricle (from the bregma: −0.2 mm AP, 1.0 mm ML, −2.0 mm DV), under isoflurane anesthesia. KA was injected 24 h later in artificial (a) CSF via the guide cannula (0.12 μg in 4 μL). Sham controls received 4 μL aCSF. Seizure behavior was monitored by modified Racine scale, as follows (Eyo et al., 2014; Racine, 1972): 1, freezing behavior; 2, rigid posture with raised tail; 3, continuous head bobbing and forepaw shaking; 4, rearing, falling, and jumping; 5, continuous level 4; 6, loss of posture and generalized convulsion activity. Mice progressing to stage 3 or more were euthanized (1, 3, or 7 days after seizure onset).

2.3 | Electroencephalography (EEG) recording and analysis

EEG recording was performed as described previously (Tian et al., 2017)), with four stainless steel electrode screws (Pinnacle Technology, Lawrence, KS) implanted through skull burr holes and attached to a microplug, and electrodes and an intracerebroventricular (ICV) guide cannula affixed with dental cement. Baseline EEG was recorded 7–14 days later, for comparison with EEG recorded post status epilepticus induction. A seizure spike was defined as a high-frequency, high-voltage synchronized poly spike or paroxysmal sharp waves with amplitude > 2-fold higher than background and lasting > 6 s. Spike number were counted by MATLAB (R2019b, the code version is SPKDT v1.0.4, which can be obtained from the original author. Sirenia® Acquisition and Sirenia® Seizure Pro (Pinnacle Technology) were used for EEG recording and seizure duration analysis, the sample rate of EEG recording was 400Hz, and the high pass filtered at 1 Hz, all EEG data were verified by manual screen additionally.

2.4 | Microglia ablation

Chow containing colony-stimulating factor 1 receptor (CSF1) inhibitor PLX3397 (600mg/kg, Chemgood company) and control chow were made by Research Diets Inc. (Elmore et al., 2014). All mice initially received control chow; for some, PLX3397 chow was substituted on day 8 for the remainder of the experiment; KA was injected 7 d after PLX3397 chow feeding. Efficacy of microglial ablation was assessed by immunostaining brain tissue sections at selected times.

2.5 | Tissue collection and immunohistochemical staining:

At intervals post-KA, mice deeply anesthetized with isoflurane were perfused with 25 mL PBS followed by 25 mL chilled formaldehyde (4%, LabChem, Zelienople, PA). Brains were removed, post-fixed with 4% formaldehyde overnight at 4°C, transferred to 30% sucrose in PBS for 72 h, and cryosectioned (17 μm thick, 30 μm thick for more interaction details in confocal images; Leica Biosystems, Wetziar, Germany). Sample sections were prepared on gelatin-coated glass slides. Sections were blocked for 60 min with 5% goat serum in Tris-buffered saline (TBS) containing 0.4% Triton X-100 (Sigma-Aldrich), then incubated 16 h at 4°C with primary IgG: rabbit anti-Iba1 (1:500, Abcam, Cambridge, UK), mouse anti-GFAP (1:500, Cell Signaling, USA), rabbit anti-NeuN (1:500, Abcam, Cambridge, UK), rabbit anti-Ki67 (1:500, Abcam, Cambridge, UK), rat anti-C3 (1:500, Abcam, Cambridge, UK), mouse anti-C1q (1:200, Abcam, Cambridge, UK), and rabbit anti-CD68 (1:500, Abcam, Cambridge, UK). After TBS wash, sections were incubated (60 min at 22°C) with corresponding fluorochrome-conjugated secondary antibodies (1:500, Life Technologies, USA). After final TBS wash, sections were mounted with Fluoromount-G DAPI (Southern Biotech, USA).

Sections (three sections per mouse) were imaged by fluorescence microscopy (EVOS FL Cell Imaging System, Life Technologies, or BZ-X810 Fluorescence Microscope, Keyence, USA or confocal LSM510, Carl Zeiss Microscopy GmbH, Jena, Germany). For EVOS microscope system, all the exposure time and gain were kept constant for all images of each experiment, and the white balance is auto-adjusted by the system. For the confocal microscopy, the pixel size was 0.27 * 0.27μm^2, Z step is 1μm. We collected 15–20 z-steps per image for representative confocal images. All the analysis was done on the whole image of the high-power field. Cell numbers and fluorescence signal intensities were quantified using ImageJ v1.52r (Fiji). Co-localized protein fluorescence immunoreactivities were quantified by ImageJ with the “Coloc 2” plugin (Release 3.0, 2017). We chose “Channel 1 Integrated (Sum) intensity” and “Manders’ tM2 value (above autothreshold of Ch1)” to calculate interaction intensity for line diagrams(Manders, Verbeek, & Aten, 1993). For the Venn diagram, the microglia Iba1 intensity, astrocyte intensity and interaction intensity calculated by Coloc 2 were used, the area of each circle in Venn diagram represents the relative value of each channel.

2.6 | Fluoro-Jade C staining

Degenerating neuronal cell bodies were identified by Fluoro-Jade C (FJC) staining (Schmued, Stowers, Scallet, & Xu, 2005): air-dried tissue sections were immersed in 0.6% potassium permanganate for 10 min, washed, immersed in a 0.001% FJC solution (Millipore, Temecula, CA) for 10 min, washed again, dehydrated and cleared with xylene, then mounted. The numbers of FJC^+ cells in the hippocampus (three sections per mouse) are reported as average number of FJC^+ of hippocampal CA3 per brain section.

2.7 | Nissl staining

Tissue sections were stained with 0.5% cresyl violet (Tian et al., 2017). The number of CA3 pyramidal neurons in a defined area was counted in at least three sections per mouse brain. The numbers of $Nissl^+$ cells in the hippocampus are reported as average number of $Nissl^+$

cells of Hipp CA3 region per brain section. All assessments of histological sections were performed in blinded fashion.

2.8 | Western blot analysis:

At stated time points, freshly dissected hippocampal tissues were homogenized in lysis buffer containing protease and phosphatase inhibitors and clarified by centrifugation (7000 g, 15 min at 4°C). Supernatant protein concentration was determined by Bradford assay, and 30 μg was loaded on to polyacrylamide gel (SDS-PAGE). Electrophoretically separated proteins were transferred to PVDF membrane (Bio-Rad). After blocking 1 h with 5% non-fat dry milk in TBST, the membrane was incubated 16 h at 4°C with rabbit anti-Iba1 (1:500, Wako Chemicals, Osaka, Japan), mouse anti-GFAP (1:500, Cell Signaling, USA), or rat anti-GAPDH (1:10000, Jackson ImmunoResearch, USA), washed with TBS, then exposed to appropriate HL-conjugated secondary antibody (1:10,000, Jackson ImmunoResearch, USA), washed again with TBS, and developed by enhanced chemiluminescence. Specific protein bands were evaluated by apparent molecular size. Images were captured and the optical density of each band was determined using ImageJ ver1.52r.

2.9 | Statistical analysis

Quantitative data are expressed as mean ± SEM. Comparison between two groups was made using Student unpaired *t* test, assuming equal variance. Multiple group comparisons were made using one-way ANOVA, or two-way ANOVA for seizure score to establish significance. All statistical tests were performed using GraphPad Prism 8.0. The significance of differences was indicated by asterisks, with * $p < 0.05$, ** $p < 0.01$, and *** $p < 0.001$.

3 | RESULTS

3.1 | Interaction between microglia and astrocytes following status epilepticus.

Gliosis is an established characteristic of rodent seizure models (Feng et al., 2019). To determine the cellular and molecular mechanisms underlying gliosis, we induced SE in WT mice via intracerebroventricular (ICV) injection of KA. Artificial CSF (aCSF) was injected into control mice (Fig. 1A). In this acute seizure model, mice present at least stage 3 seizure activity on a modified Racine scale, with continuous head bobbing and forepaw shaking signifying the onset of seizures. Some mice were monitored by EEG to confirm seizure onset (Fig. 1B). CA3 area of hippocampal tissue sections from control mice and mice with KA-induced seizures were examined by immunofluorescence staining, with Iba1 immunoreactivity serving as a marker for microglia, and GFAP for astrocytes. Both immunoreactivities were significantly increased at days 3 and 7 post-KA when compared to controls (Fig. 1C–E). Western blot evaluation of hippocampal tissues at 12 h, 1 d, 2 d, and 3 d post-KA injection (Fig. 1F) revealed that starting at 1 d, the Iba1 content was 2-fold higher than in aCSF control recipients (Fig. 1G), while the GFAP content (Fig.1H) was not significantly greater than in controls until 3 d after SE onset.

A remarkable visual overlapping between Iba1 and GFAP immunoreactivities was commonly observed in the KA-treated group but rarely in controls. The close spatial relationship between microglia and astrocytes, revealed by confocal imaging, suggested that

microglia-astrocyte physical interaction occurred following status epilepticus (Fig. 2A). Venn and line diagrams further quantified the co-localization (Fig. 2B, C). Taken together, our results infer a sequential activation of microglia and astrocytes, and that these cell types interact in response to KA-induced seizures.

3.2 | Microglial ablation reduces astrocyte activation

Since activation was apparent earlier in microglia than in astrocytes, in response to KA-induced seizures, we next investigated whether microglial ablation would affect astrogliosis. We employed PLX3397, an antagonist of colony-stimulating factor 1 receptor (CSF1R) administered in chow, to deplete microglia (Fig. 3A), as described previously (Elmore et al., 2014). By contrast to the control chow group, Iba1$^+$ cells were largely absent in PLX3397 recipients at both 3 d and 7d after status epilepticus. This indicated successful ablation (Fig. 3B, D, F). Interestingly, the number of GFAP$^+$ cells in the PLX3397 group also was significantly lower than in the control chow group (Fig. 3B, C, E). These results suggest that KA-induced astrocyte activation was dramatically reduced when microglia were depleted.

Next, using C3 as a marker of activated astrocytes, we studied the effect of microglia ablation on the gliotic response to KA-induced status epilepticus. C3 is highly expressed by A1 astrocytes, a potentially neurotoxic type of activated astrocyte (Liddelow et al., 2017). Cytoplasmic C3 immunoreactivity was highly elevated in GFAP$^+$ astrocytes of control chow recipient mice at 3 d and 7 d after KA injection (Fig. 3G, H). By contrast, the level of C3 immunoreactivity was significantly lower in GFAP$^+$ astrocytes of PLX3397 recipients following KA injection (Fig. 3G, H). We found additionally that, by comparison with the control chow group, microglial ablation significantly reduced the number of astrocytes expressing the proliferation marker Ki67 following seizure induction (Fig. 3I, J). These results are consistent with KA-induced astrocyte activation and proliferation being suppressed by microglial ablation.

3.3 | Microglial activation is reduced in the absence of C3 or the C3a receptor

Having demonstrated that microglia are required for astrocyte activation after seizures, we next investigated whether there was a reciprocal interaction. Several recent studies have implicated complement components in the pathophysiology of epilepsy, in both humans and mice (Aronica et al., 2007; Schartz et al., 2018; Wyatt et al., 2017). Our results showed that astrocytic C3 production is upregulated following status epilepticus. Furthermore, microglial expression of the canonical receptor for C3a (C3aR), the soluble signaling cleavage fragment of C3, is reported to be increased in several disease models (L. Y. Zhang et al., 2020). It is plausible that the observed microglia-astrocyte interaction following KA-induced status epilepticus is mediated in part by the C3-C3aR pathway. We therefore recorded seizure scores and EEG, and compared between WT, C3$^{-/-}$, and C3aR$^{-/-}$ mice after ICV KA injection (Fig. 4A). Seizure scores (Fig. 4B) and EEG activity (Fig. 4C–E) for the three genotypes did not differ significantly. We next investigated expression of C1q, the initiating component of the classical complement pathway, and marker for microglial activation (Liddelow et al., 2017). As anticipated, C1q largely co-localized with Iba1 and greatly increased in WT mice 1 d, 3 d and 7 d after status epilepticus (Fig. 5A–C, Supplementary Figure 2A–B). However, C3 expression and GFAP$^+$ cell number was not upregulated

significantly until 3 d after status epilepticus (Supplementary Figure 2D–F). CD68, a lysosomal marker of phagocytic cells, is highly co-localized with Iba1^{+} and Cx3cr1-GFP microglia after status epilepticus (Supplementary Figure 4A–B). We found that CD68 expression was markedly suppressed in both C3$^{-/-}$ and C3aR$^{-/-}$ mice on day 7 after seizures by comparison with WT KA-injected mice (Fig. 5D–E), further verified the reduction of microglial activation. These complementary results indicate an important role for the C3-C3aR axis in the activation of microglia that follows status epilepticus.

3.4 | C3-C3aR signaling is required for gliosis formation and mediates microglia-astrocyte interaction

After demonstrating the importance of the C3-C3aR pathway for microglial activation, we next investigated whether this signaling pathway mediates KA-induced gliosis and microglia-astrocyte interaction. First, we examined microglia-astrocyte interaction in WT, C3$^{-/-}$ and C3aR$^{-/-}$ mice before KA-induced seizure. Our results showed that there was no difference between these mice in Iba1^{+} area (%), GFAP^{+} area (%), or iba1 and GFAP colocalization intensity (Supplementary Figure 3). However, after KA injection, we found that fewer Iba1^{+} microglia and GFAP^{+} astrocytes in brain lesions of both C3$^{-/-}$ and C3aR$^{-/-}$mice by comparison with WT KA-injected control mice (Fig. 6A–C). Furthermore, the areas of Iba1 and GFAP staining overlap were significantly smaller in C3$^{-/-}$ and C3aR$^{-/-}$ mice (Fig. 6A, D, E). These results support our conclusion that astrocytic C3 interacts with microglial C3aR and plays a pivotal role in the crosstalk between these two glial cell types, promoting seizure-induced gliosis.

3.5 | C3-C3aR pathway mediates neurodegeneration associated with epilepsy

To investigate the functional consequence of C3-C3aR signaling we evaluated post-seizure weight loss and neurodegeneration in the hippocampal CA3 region of WT, C3$^{-/-}$, and C3aR$^{-/-}$ mice 7 d after KA injection. Epileptic rodents rapidly lose 10–20% body weight, then gradually recover in the following days (Varvel et al., 2016). As predicted, we observed approximately 15% weight loss in KA-treated WT mice 1 day after SE, with weight regain beginning on day 3 post-KA, reaching original weight on day 7. However, weight loss was minimal in KA-injected mice deficient in C3 or C3aR (Fig. 7A, B). We compared the neuropathology of different mouse groups histochemically (Nissl) and immunohistochemically (NeuN). By comparison to aCSF-recipient WT mice at d 7, numbers of Nissl^{+} and NeuN^{+} neurons were substantially fewer in KA recipient WT mice. However, comparison of WT and C3$^{-/-}$ and C3aR$^{-/-}$ mice 7 days post-KA revealed Nissl^{+} and NeuN^{+} neurons were significantly more numerous in C3$^{-/-}$, but not in C3aR$^{-/-}$ genotypes (Fig. 7C–F). Using Fluoro Jade C (FJC) staining to evaluate the extent of neurodegeneration following KA injection, we observed significantly fewer FJC^{+} neurons in the hippocampal CA3 region of C3$^{-/-}$ mice by comparison with KA-injected WT mice (Fig. 7C–F). However, in contrast to C3$^{-/-}$ mice, C3aR$^{-/-}$ mice did not show significant neuronal degeneration when compared to WT. These results demonstrate that at minimum C3$^{-/-}$ can rescue KA-induced neurodegeneration, and suggest importance of C3 signaling for KA-induced neuronal damage.

4 | DISCUSSION

The present study extends our investigations of the potential role of glial cells in epilepsy (Eyo et al., 2017; Eyo et al., 2014; Feng et al., 2019). By combining pharmacologic and genetic tools, we demonstrate that, following a single episode of status epilepticus induced by intracerebroventricular KA injection, C3-C3aR signaling between microglia and astrocytes contributes to neurodegeneration. Specifically, microglia activated by status epilepticus promoted astrocytes to adopt a neurotoxic (A1) phenotype in which they upregulate complement C3 production. Secreted C3 (presumably via its C3a cleavage product) further activated microglia, thus establishing a vicious cycle amplifying KA-induced gliosis and promoting neurodegeneration (Fig. 8). Ablation of microglia and deficiency of C3 signaling attenuated the gliosis and neurodegeneration that follows status epilepticus. Our study has revealed that C3 signaling mediates crosstalk between astrocytes and microglia in seizure pathogenesis.

4.1 | Activated microglia trigger astrogliosis following status epilepticus

Microglial activation is observed in various animal models of epilepsy (Bosco et al., 2018; Eyo et al., 2017), and astrocytes with distinct morphological and functional characteristics are thought also to play an active role in epilepsy pathogenesis (Hubbard, Szu, Yonan, & Binder, 2016; Seifert & Steinhauser, 2013). In agreement with previous studies, we demonstrated that both microglia and astrocytes are activated following induction of status epilepticus by KA. Microglial activation (evidenced by enhanced Iba1 and C1q immunoreactivities) was apparent at 24 hours, and at day 3 there was significant activation of astrocytes strongly expressing GFAP and C3, suggesting A1 phenotype (upregulated expression of classical complement cascade genes, and destructive to synapses). Astrocytes of A2 phenotype (considered protective) upregulate many neurotrophic factors (Liddelow et al., 2017). Gliosis is a commonly acknowledged histopathological hallmark of idiopathic and acquired epilepsies (Feng et al., 2019; Sofroniew & Vinters, 2010). Our finding that microglial ablation by oral administration of PLX3397 reduced astrogliosis, suggests that microglia trigger secondary astrocyte reactivity following seizures. Previous studies have reported that pro-inflammatory cytokines and chemokines released by activated microglia (e.g., interleukin (IL)-1, IL-6, IL-8, and tumor necrosis factor alpha (TNF-α); (Barron, 1995), are important for gliosis formation. In addition to IL-1 and TNF-α, microglia-derived C1q is critical for astrocytic adoption of the neurotoxic A1 phenotype (Liddelow & Barres, 2017). Our finding that reactive microglia express high levels of C1q after seizure activity is consistent with that prediction. Future studies need to directly test the function of microglial C1q in mediating microglial-dependent astrocyte activation following seizures. However, we should be aware that, functional changes in astrocytes, such as impairment of astrocyte coupling, occurs within a few hours after status epilepticus (Bedner et al., 2015). In addition, astrocyte Ca^{2+} activities are more closely to neuronal activity than microglia Ca^{2+} (Paukert et al., 2014; Stobart et al., 2018; Umpierre et al., 2020). These results suggest the potential signaling from astrocytes to microglia in response to seizure activity.

4.2 | Complement C3-C3aR pathway in microglia-astrocyte interaction.

Although status epilepticus caused significant increase in the interaction between microglia and astrocytes, the underlying means of signaling remain largely unknown. Complement factors, a key component of the immune system, are now recognized to have functions beyond host defense. Cleavage of the C3 protein is a critical step in diverse effector functions (Satyam et al., 2017; van Beek, Elward, & Gasque, 2003). Elevated complement C3 has previously been reported in human epilepsy disorders, including focal cortical dysplasia (Wyatt et al., 2017), temporal lobe epilepsy (Aronica et al., 2007) and tuberous sclerosis complex (Boer et al., 2006), as well as in experimental status epilepticus induced in mice by injection of KA (Schartz et al., 2018) or pilocarpine (Kharatishvili et al., 2014). Of particular note, mice genetically deficient in C3 have been reported largely resistant to seizures induced by acute viral infections (Libbey, Kirkman, Wilcox, White, & Fujinami, 2010; Vezzani et al., 2016). Consistent with those studies, we found that cytoplasmic C3 immunoreactivity in astrocytes was significantly increased in the hippocampus CA3 region after KA-induced status epilepticus. We then tested, for the first time, the hypothesis that status epilepticus activates microglia to secondarily activate astrocytes which in turn secrete C3 to reciprocally activate microglia via C3aR signaling. Our data suggest a vicious cycle promoting gliosis. This interpretation of the data, supported by loss of function genetic models including $C3^{-/-}$ and $C3aR^{-/-}$ mice, suggests that therapeutic interruption of C3-C3aR signaling could substantially ameliorate gliosis. One caveat in our study is that we used the co-localization of Iba1 and GFAP staining to examine microglia-astrocyte interaction. Since both Iba1 and GFAP are up-regulated as well as their numbers are increased after seizures, the methodology may increase the probability to detect these markers in thin processes of glia. Therefore, the interaction between microglia and astrocytes after seizures is likely over-estimated compared to control animals. Future studies using better markers or genetic labelling are needed to address this potential caveat.

4.3 | C3-C3aR pathway in neurodegeneration.

Epilepsy is commonly accompanied by neurodegenerative and pathological alterations to neuronal circuits in affected brain regions. This study revealed significant attenuation of histochemically evident neurodegeneration in the absence of C3. It is curious that mice lacking C3a receptors were not significantly spared neurodegeneration following status epilepticus. Possible reasons for this observation include: (1) C1q from activated microglia serves as an “eat me” signal to mediate microglial phagocytic responses (Barnum, 2017; Schafer et al., 2012; Schafer, Lehrman, & Stevens, 2013; Wagner & Frank, 2010). (2) Reactive A1 astrocytes can upregulate multiple complement genes, including C3, whose cleavage products, such as iC3b, are destructive to synapses and secrete neurotoxins (Liddelow & Barres, 2017). (3) Neurotoxic A1 astrocytes also secrete pro-inflammatory factors (including IL-1β, TNF-α and NO) and cytotoxins during gliosis (Liddelow & Barres, 2017). The observed discrepancy in KA-induced neurodegeneration between $C3^{-/-}$ mice and $C3aR^{-/-}$ mice, implies that the second possibility may be correct. C3 cleavage also generates C3b, which has been shown to correlate with apoptotic neurons through CR3 (Elward & Gasque, 2003). Furthermore, C3b production would also lead to cleavage of C5, which can contribute to neuroinflammation in epilepsy (Leslie & Mayor, 2013; Schartz et al., 2018).

Future studies should investigate these possibilities and further examine how complement cascades are involved in KA-induced neurodegeneration.

5 | CONCLUSIONS

Our study documents both spatial and temporal crosstalk between microglia and astrocytes through the C3-C3aR pathway following KA-induced seizures. The findings enhance understanding of the dynamic interactions between microglia and astrocytes and the genesis of gliosis and neurodegeneration in the wake of status epilepticus. The results have therapeutic implications. Future studies should address how the C3-C3aR pathway contributes to the pathology associated with status epilepticus and which complement components would be optimal to neutralize for therapeutic purposes.

Supplementary Material

Refer to Web version on PubMed Central for supplementary material.

ACKNOWLEDGMENTS

This work is supported by the National Institutes of Health (R01NS088627, R01NS112144) to L.J.W., and the National Natural Science Foundation of China (81601142) to Y.W. We thank Ann B. Peterson (Mayo Clinic) for language editing and all member of the Wu laboratory at Mayo Clinic for insightful discussions.

REFERENCES

Aronica E, Boer K, van Vliet EA, Redeker S, Baayen JC, Spliet WG,…Gorter JA (2007). Complement activation in experimental and human temporal lobe epilepsy. Neurobiol Dis, 26(3), 497–511. doi:10.1016/j.nbd.2007.01.015 [PubMed: 17412602]

Barnum SR (2017). Complement: A primer for the coming therapeutic revolution. Pharmacol Ther, 172, 63–72. doi:10.1016/j.pharmthera.2016.11.014 [PubMed: 27914981]

Barron KD (1995). The microglial cell. A historical review. J Neurol Sci, 134 Suppl, 57–68. doi:10.1016/0022-510x(95)00209-k

Bedner P, Dupper A, Huttmann K, Muller J, Herde MK, Dublin P,…Steinhauser C (2015). Astrocyte uncoupling as a cause of human temporal lobe epilepsy. Brain, 138(Pt 5), 1208–1222. doi:10.1093/brain/awv067 [PubMed: 25765328]

Boer K, Spliet WG, van Rijen PC, Redeker S, Troost D, & Aronica E (2006). Evidence of activated microglia in focal cortical dysplasia. J Neuroimmunol, 173(1–2), 188–195. doi:10.1016/j.jneuroim.2006.01.002 [PubMed: 16483671]

Bosco DB, Zheng J, Xu Z, Peng J, Eyo UB, Tang K,…Wu LJ (2018). RNAseq analysis of hippocampal microglia after kainic acid-induced seizures. Mol Brain, 11(1), 34. doi:10.1186/s13041-018-0376-5 [PubMed: 29925434]

Chavan SS, Pavlov VA, & Tracey KJ (2017). Mechanisms and Therapeutic Relevance of Neuro-immune Communication. Immunity, 46(6), 927–942. doi:10.1016/j.immuni.2017.06.008 [PubMed: 28636960]

Chen T, Lennon VA, Liu YU, Bosco DB, Li Y, Yi MH,…Wu LJ (2020). Astrocyte-microglia interaction drives evolving neuromyelitis optica lesion. J Clin Invest, 130(8), 4025–4038. doi:10.1172/JCI134816 [PubMed: 32568214]

Chu Y, Jin X, Parada I, Pesic A, Stevens B, Barres B, & Prince DA (2010). Enhanced synaptic connectivity and epilepsy in C1q knockout mice. Proc Natl Acad Sci U S A, 107(17), 7975–7980. doi:10.1073/pnas.0913449107 [PubMed: 20375278]

Davoust N, Jones J, Stahel PF, Ames RS, & Barnum SR (1999). Receptor for the C3a anaphylatoxin is expressed by neurons and glial cells. Glia, 26(3), 201–211. doi:10.1002/(sici)1098-1136(199905)26:3<201::aid-glia2>3.0.co;2-m [PubMed: 10340761]

Deshpande T, Li T, Henning L, Wu Z, Muller J, Seifert G,…Bedner P (2020). Constitutive deletion of astrocytic connexins aggravates kainate-induced epilepsy. Glia, 68(10), 2136–2147. doi:10.1002/glia.23832 [PubMed: 32240558]

Elmore MR, Najafi AR, Koike MA, Dagher NN, Spangenberg EE, Rice RA,…Green KN (2014). Colony-stimulating factor 1 receptor signaling is necessary for microglia viability, unmasking a microglia progenitor cell in the adult brain. Neuron, 82(2), 380–397. doi:10.1016/j.neuron.2014.02.040 [PubMed: 24742461]

Elward K, & Gasque P (2003). “Eat me” and “don’t eat me” signals govern the innate immune response and tissue repair in the CNS: emphasis on the critical role of the complement system. Mol Immunol, 40(2–4), 85–94. doi:10.1016/s0161-5890(03)00109-3 [PubMed: 12914815]

Eyo UB, Gu N, De S, Dong H, Richardson JR, & Wu LJ (2015). Modulation of microglial process convergence toward neuronal dendrites by extracellular calcium. J Neurosci, 35(6), 2417–2422. doi:10.1523/JNEUROSCI.3279-14.2015 [PubMed: 25673836]

Eyo UB, Murugan M, & Wu LJ (2017). Microglia-Neuron Communication in Epilepsy. Glia, 65(1), 5–18. doi:10.1002/glia.23006 [PubMed: 27189853]

Eyo UB, Peng J, Swiatkowski P, Mukherjee A, Bispo A, & Wu LJ (2014). Neuronal Hyperactivity Recruits Microglial Processes via Neuronal NMDA Receptors and Microglial P2Y12 Receptors after Status Epilepticus. J Neurosci, 34(32), 10528–10540. doi:10.1523/JNEUROSCI.0416-14.2014 [PubMed: 25100587]

Feng L, Murugan M, Bosco DB, Liu Y, Peng J, Worrell GA,…Wu LJ (2019). Microglial proliferation and monocyte infiltration contribute to microgliosis following status epilepticus. Glia, 67(8), 1434–1448. doi:10.1002/glia.23616 [PubMed: 31179602]

Hubbard JA, Szu JI, Yonan JM, & Binder DK (2016). Regulation of astrocyte glutamate transporter-1 (GLT1) and aquaporin-4 (AQP4) expression in a model of epilepsy. Exp Neurol, 283(Pt A), 85–96. doi:10.1016/j.expneurol.2016.05.003 [PubMed: 27155358]

Kharatishvili I, Shan ZY, She DT, Foong S, Kurniawan ND, & Reutens DC (2014). MRI changes and complement activation correlate with epileptogenicity in a mouse model of temporal lobe epilepsy. Brain Struct Funct, 219(2), 683–706. doi:10.1007/s00429-013-0528-4 [PubMed: 23474541]

Kipnis J (2016). Multifaceted interactions between adaptive immunity and the central nervous system. Science, 353(6301), 766–771. doi:10.1126/science.aag2638 [PubMed: 27540163]

Leslie JD, & Mayor R (2013). Complement in animal development: unexpected roles of a highly conserved pathway. Semin Immunol, 25(1), 39–46. doi:10.1016/j.smim.2013.04.005 [PubMed: 23665279]

Lian H, Yang L, Cole A, Sun L, Chiang AC, Fowler SW,…Zheng H (2015). NFkappaB-activated astroglial release of complement C3 compromises neuronal morphology and function associated with Alzheimer’s disease. Neuron, 85(1), 101–115. doi:10.1016/j.neuron.2014.11.018 [PubMed: 25533482]

Libbey JE, Kirkman NJ, Wilcox KS, White HS, & Fujinami RS (2010). Role for complement in the development of seizures following acute viral infection. J Virol, 84(13), 6452–6460. doi:10.1128/JVI.00422-10 [PubMed: 20427530]

Liddelow SA, & Barres BA (2017). Reactive Astrocytes: Production, Function, and Therapeutic Potential. Immunity, 46(6), 957–967. doi:10.1016/j.immuni.2017.06.006 [PubMed: 28636962]

Liddelow SA, Guttenplan KA, Clarke LE, Bennett FC, Bohlen CJ, Schirmer L,…Barres BA (2017). Neurotoxic reactive astrocytes are induced by activated microglia. Nature, 541(7638), 481–487. doi:10.1038/nature21029 [PubMed: 28099414]

Litvinchuk A, Wan YW, Swartzlander DB, Chen F, Cole A, Propson NE,…Zheng H (2018). Complement C3aR Inactivation Attenuates Tau Pathology and Reverses an Immune Network Deregulated in Tauopathy Models and Alzheimer’s Disease. Neuron, 100(6), 1337–1353 e1335. doi:10.1016/j.neuron.2018.10.031 [PubMed: 30415998]

Manders EMM, Verbeek FJ, & Aten JA (1993). Measurement of co-localization of objects in dual-colour confocal images. Journal of Microscopy, 169(3), 375–382. doi:10.1111/j.1365-2818.1993.tb03313.x

Patel DC, Tewari BP, Chaunsali L, & Sontheimer H (2019). Neuron-glia interactions in the pathophysiology of epilepsy. Nat Rev Neurosci, 20(5), 282–297. doi:10.1038/s41583-019-0126-4 [PubMed: 30792501]

Paukert M, Agarwal A, Cha J, Doze VA, Kang JU, & Bergles DE (2014). Norepinephrine controls astroglial responsiveness to local circuit activity. Neuron, 82(6), 1263–1270. doi:10.1016/j.neuron.2014.04.038 [PubMed: 24945771]

Racine RJ (1972). Modification of seizure activity by electrical stimulation. II. Motor seizure. Electroencephalogr Clin Neurophysiol, 32(3), 281–294. [PubMed: 4110397]

Robel S (2017). Astroglial Scarring and Seizures: A Cell Biological Perspective on Epilepsy. Neuroscientist, 23(2), 152–168. doi:10.1177/1073858416645498 [PubMed: 27118807]

Robel S, Buckingham SC, Boni JL, Campbell SL, Danbolt NC, Riedemann T,…Sontheimer H (2015). Reactive astrogliosis causes the development of spontaneous seizures. J Neurosci, 35(8), 3330–3345. doi:10.1523/JNEUROSCI.1574-14.2015 [PubMed: 25716834]

Satyam A, Kannan L, Matsumoto N, Geha M, Lapchak PH, Bosse R,…Tsokos GC (2017). Intracellular Activation of Complement 3 Is Responsible for Intestinal Tissue Damage during Mesenteric Ischemia. J Immunol, 198(2), 788–797. doi:10.4049/jimmunol.1502287 [PubMed: 27913632]

Schafer DP, Lehrman EK, Kautzman AG, Koyama R, Mardinly AR, Yamasaki R,…Stevens B (2012). Microglia sculpt postnatal neural circuits in an activity and complement-dependent manner. Neuron, 74(4), 691–705. doi:10.1016/j.neuron.2012.03.026 [PubMed: 22632727]

Schafer DP, Lehrman EK, & Stevens B (2013). The “quad-partite” synapse: Microglia-synapse interactions in the developing and mature CNS. Glia, 61(1), 24–36. doi:10.1002/glia.22389 [PubMed: 22829357]

Schartz ND, Wyatt-Johnson SK, Price LR, Colin SA, & Brewster AL (2018). Status epilepticus triggers long-lasting activation of complement C1q-C3 signaling in the hippocampus that correlates with seizure frequency in experimental epilepsy. Neurobiol Dis, 109(Pt A), 163–173. doi:10.1016/j.nbd.2017.10.012 [PubMed: 29074125]

Schmued LC, Stowers CC, Scallet AC, & Xu L (2005). Fluoro-Jade C results in ultra high resolution and contrast labeling of degenerating neurons. Brain Res, 1035(1), 24–31. doi:10.1016/j.brainres.2004.11.054 [PubMed: 15713273]

Seifert G, & Steinhauser C (2013). Neuron-astrocyte signaling and epilepsy. Exp Neurol, 244, 4–10. doi:10.1016/j.expneurol.2011.08.024 [PubMed: 21925173]

Shapiro LA, Wang L, & Ribak CE (2008). Rapid astrocyte and microglial activation following pilocarpine-induced seizures in rats. Epilepsia, 49 Suppl 2, 33–41. doi:10.1111/j.1528-1167.2008.01491.x

Sofroniew MV (2009). Molecular dissection of reactive astrogliosis and glial scar formation. Trends Neurosci, 32(12), 638–647. doi:10.1016/j.tins.2009.08.002 [PubMed: 19782411]

Sofroniew MV, & Vinters HV (2010). Astrocytes: biology and pathology. Acta Neuropathol, 119(1), 7–35. doi:10.1007/s00401-009-0619-8 [PubMed: 20012068]

Stobart JL, Ferrari KD, Barrett MJP, Gluck C, Stobart MJ, Zuend M, & Weber B (2018). Cortical Circuit Activity Evokes Rapid Astrocyte Calcium Signals on a Similar Timescale to Neurons. Neuron, 98(4), 726–735 e724. doi:10.1016/j.neuron.2018.03.050 [PubMed: 29706581]

Szalay G, Martinecz B, Lenart N, Kornyei Z, Orsolits B, Judak L,…Denes A (2016). Microglia protect against brain injury and their selective elimination dysregulates neuronal network activity after stroke. Nat Commun, 7, 11499. doi:10.1038/ncomms11499 [PubMed: 27139776]

Thijs RD, Surges R, O’Brien TJ, & Sander JW (2019). Epilepsy in adults. Lancet, 393(10172), 689–701. doi:10.1016/S0140-6736(18)32596-0 [PubMed: 30686584]

Tian DS, Peng J, Murugan M, Feng LJ, Liu JL, Eyo UB,…Wu LJ (2017). Chemokine CCL2-CCR2 Signaling Induces Neuronal Cell Death via STAT3 Activation and IL-1beta Production after Status Epilepticus. J Neurosci, 37(33), 7878–7892. doi:10.1523/JNEUROSCI.0315-17.2017 [PubMed: 28716963]

Umpierre AD, Bystrom LL, Ying Y, Liu YU, Worrell G, & Wu LJ (2020). Microglial calcium signaling is attuned to neuronal activity in awake mice. Elife, 9. doi:10.7554/eLife.56502

van Beek J, Elward K, & Gasque P (2003). Activation of complement in the central nervous system: roles in neurodegeneration and neuroprotection. Ann N Y Acad Sci, 992, 56–71. [PubMed: 12794047]

Varvel NH, Neher JJ, Bosch A, Wang W, Ransohoff RM, Miller RJ, & Dingledine R (2016). Infiltrating monocytes promote brain inflammation and exacerbate neuronal damage after status epilepticus. Proc Natl Acad Sci U S A, 113(38), E5665–5674. doi:10.1073/pnas.1604263113 [PubMed: 27601660]

Vezzani A, Fujinami RS, White HS, Preux PM, Blumcke I, Sander JW, & Loscher W (2016). Infections, inflammation and epilepsy. Acta Neuropathol, 131(2), 211–234. doi:10.1007/s00401-015-1481-5 [PubMed: 26423537]

Wagner E, & Frank MM (2010). Therapeutic potential of complement modulation. Nat Rev Drug Discov, 9(1), 43–56. doi:10.1038/nrd3011 [PubMed: 19960015]

Wyatt SK, Witt T, Barbaro NM, Cohen-Gadol AA, & Brewster AL (2017). Enhanced classical complement pathway activation and altered phagocytosis signaling molecules in human epilepsy. Exp Neurol, 295, 184–193. doi:10.1016/j.expneurol.2017.06.009 [PubMed: 28601603]

Zhang D, Hu X, Qian L, O'Callaghan JP, & Hong JS (2010). Astrogliosis in CNS pathologies: is there a role for microglia? Mol Neurobiol, 41(2–3), 232–241. doi:10.1007/s12035-010-8098-4 [PubMed: 20148316]

Zhang LY, Pan J, Mamtilahun M, Zhu Y, Wang L, Venkatesh A,…Yang GY (2020). Microglia exacerbate white matter injury via complement C3/C3aR pathway after hypoperfusion. Theranostics, 10(1), 74–90. doi:10.7150/thno.35841 [PubMed: 31903107]

Zhang Y, Chen K, Sloan SA, Bennett ML, Scholze AR, O'Keeffe S,…Wu JQ (2014). An RNA-sequencing transcriptome and splicing database of glia, neurons, and vascular cells of the cerebral cortex. J Neurosci, 34(36), 11929–11947. doi:10.1523/JNEUROSCI.1860-14.2014 [PubMed: 25186741]

MAIN POINTS

1. Microglia are required for astrocytes activation in experimental status epilepticus
2. C3 from astrocytes activates microglia via C3a receptors
3. Microglia-astrocyte interaction promotes gliosis and neuronal injury after seizures

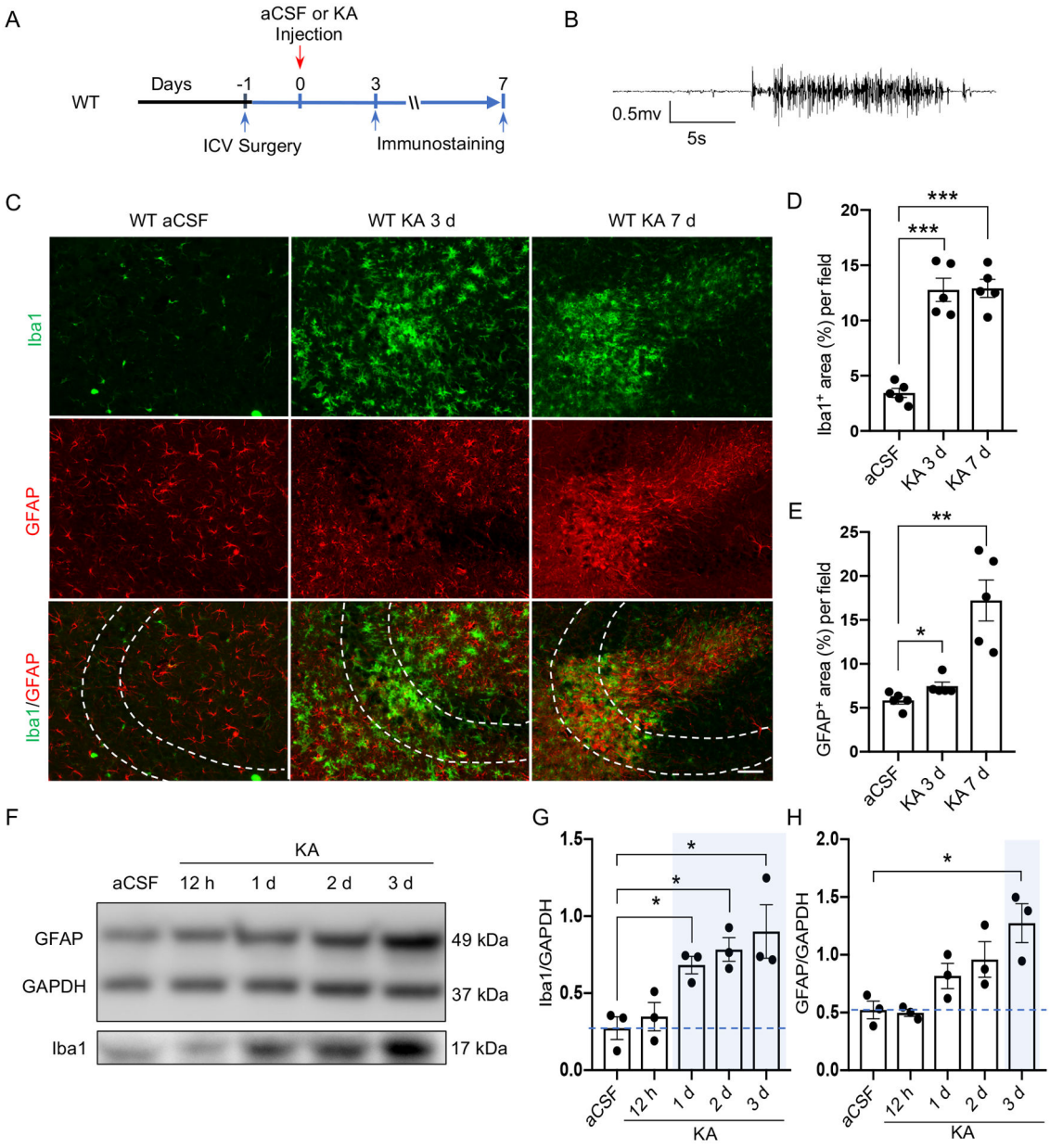

Fig. 1: Upregulation of microglia and astrocyte markers in hippocampal CA3 region of WT mice following KA-induced status epilepticus.

(A) Experimental time line. (B) Representative EEG trace from WT mouse before and after KA injection shows epileptiform burst. (C) Representative images show enhanced immunoreactivity and increasing co-localization of astrocytic and microglial markers (GFAP and Iba1) at 3 d and 7 d after ipsilateral KA injection, by comparison to aCSF injection. Scale bar: 50 μm. (D, E) Quantitation (as percentage; image J), at 3 d and 7 d after aCSF or KA injection, of the area occupied by $Iba1^+$ cells (n=5 mice per group, 3 sections per mouse, * $p<0.05$, ** $p<0.01$, *** $p<0.001$, one-way ANOVA) and $GFAP^+$ cells (n=5 mice per group, 3 sections per mouse, * $p<0.05$, ** $p<0.01$). (F) Relative ipsilateral tissue abundance (by western blot) of GFAP and Iba1 immunoreactivities at intervals after KA injection by comparison aCSF injection. GAPDH is loading control. (G, H) Densitometric analysis of

immunoreactive bands. All data are normalized to loading control (n=3–5 mice per group, * $p<0.05$, t-test).

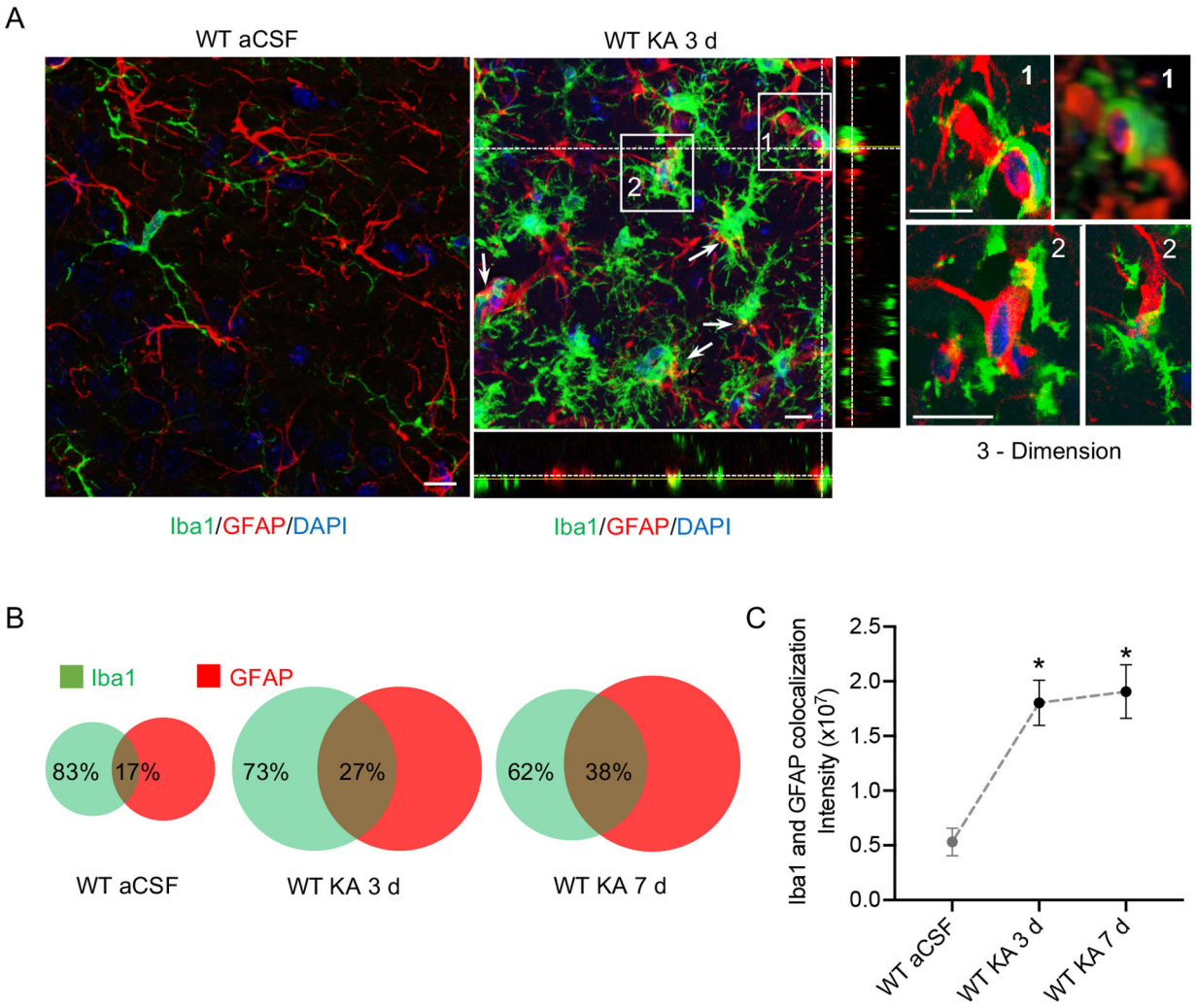

Fig. 2: Microglia and astrocyte interactions following KA-induced status epilepticus in hippocampal CA3 region of WT mice.

(A) Representative orthogonal confocal images reveal microglia-astrocyte interaction after KA injection (arrows and boxes in A) on day 3. Both soma and processes of microglia appear to directly contact astrocytes in magnified boxed areas (right). Scale bar: 10 μm. (B, C) Quantitative analysis of $Iba1^{+}/GFAP^{+}$ co-localization at days 3 and 7 after KA by comparison with aCSF recipient control group (day 3) (n=3–4 mice per group, * $p<0.05$, t-test).

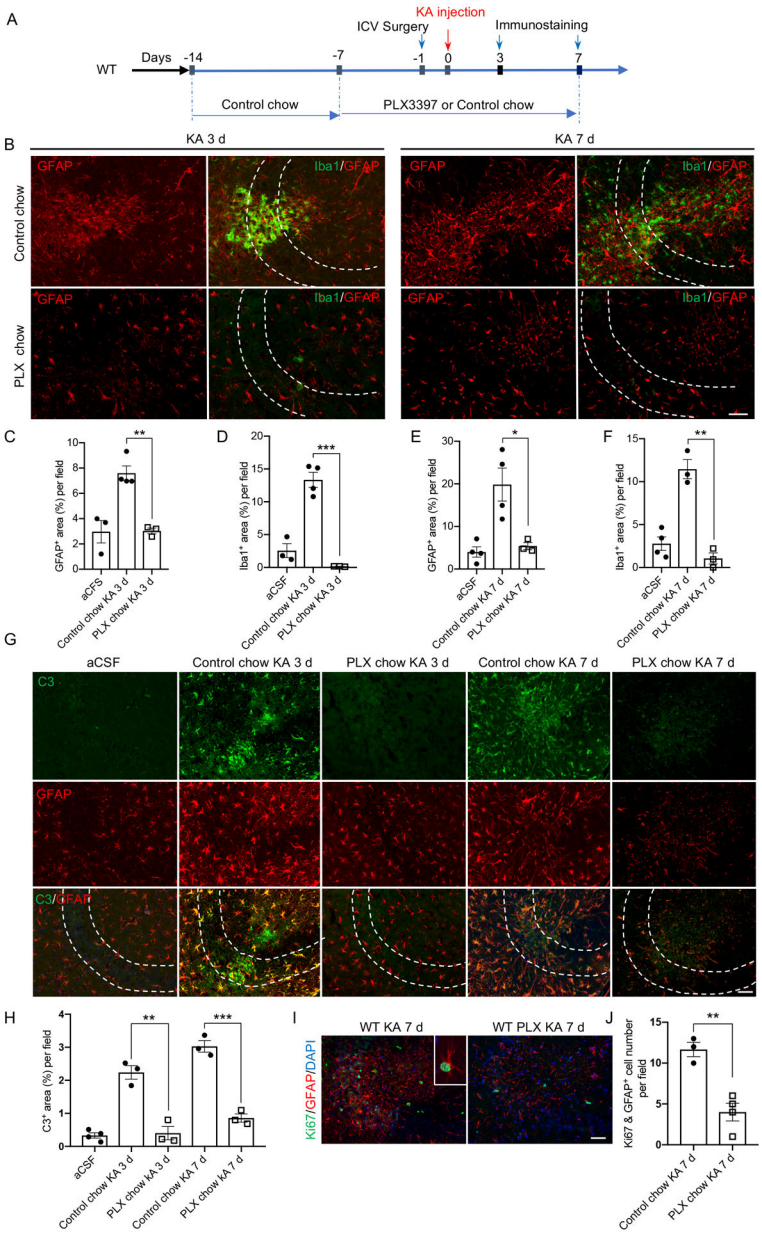

Fig. 3: Microglial depletion with a CSF1 antagonist (PLX3397) reduces astroglial proliferation and promotion of A1-type phenotype following status epilepticus.

(A) Experimental time line. (B) Representative images showing Iba1$^+$ and GFAP$^+$ cells in the hippocampus CA3 region with or without PLX3397 treatment at different time points after KA injection. Scale bar: 50 μm. (C-F) Quantitative analysis of Iba1$^+$ and GFAP$^+$ cells after KA administration. Microglial ablation reduced astrogliosis at 3 d and 7 d after status epilepticus induction (n=3–4 mice per group, 3 sections per mouse, * $p<0.05$, ** $p<0.01$, *** $p<0.001$, t-test). (G) Representative images illustrate significantly fewer A1-type (complement C3$^+$) astrocytes after microglial depletion at 3 d and 7 d. Scale bar: 50 μm. (H) Quantitative analysis of C3$^+$ astrocytes at 3 d and 7 d in CA3 of mice receiving PLX 3397 chow or control chow (n=3–4 mice per group, 3 sections per mouse, ** $p<0.05$, *** $p<0.001$, t-test). (I) Representative images showing astrocyte proliferation (dual GFAP$^+$/

Ki67$^+$ cells) at 7 d after KA administration in mice receiving PLX3397 or control chow. Scale bar: 50 μm. (J) Quantitative analysis of Ki67$^+$/GFAP$^+$ cell numbers, at 7 d after KA-induced status epilepticus (n=4, 3 sections per mouse, ** $p<0.01$, t-test).

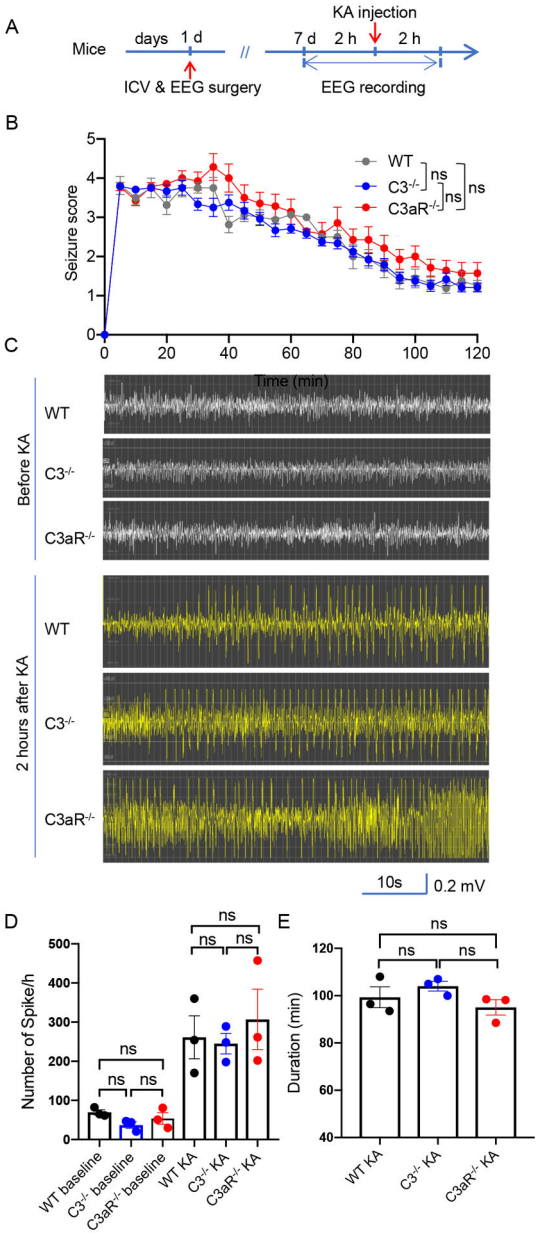

Fig. 4: Seizure activity before and after KA induced status epilepticus in WT, C3$^{-/-}$ and C3aR$^{-/-}$ mice.

(A) Experimental time line. (B) Seizure scores during intracerebroventricular injection of KA in WT (n=8), C3$^{-/-}$ (n=12) and C3aR$^{-/-}$ (n=7) mice. ns = not significant, p=0.15, two-way ANOVA. (C) Representative EEG trace from WT, C3$^{-/-}$ and C3aR$^{-/-}$ mice 2 hours before and after KA injection shows epileptiform burst. (D-E) Spike number and seizure duration(min) detected no significant difference between the WT, C3$^{-/-}$ and C3aR$^{-/-}$ mice (n=3 for each group, ns = not significant, one-way ANOVA).

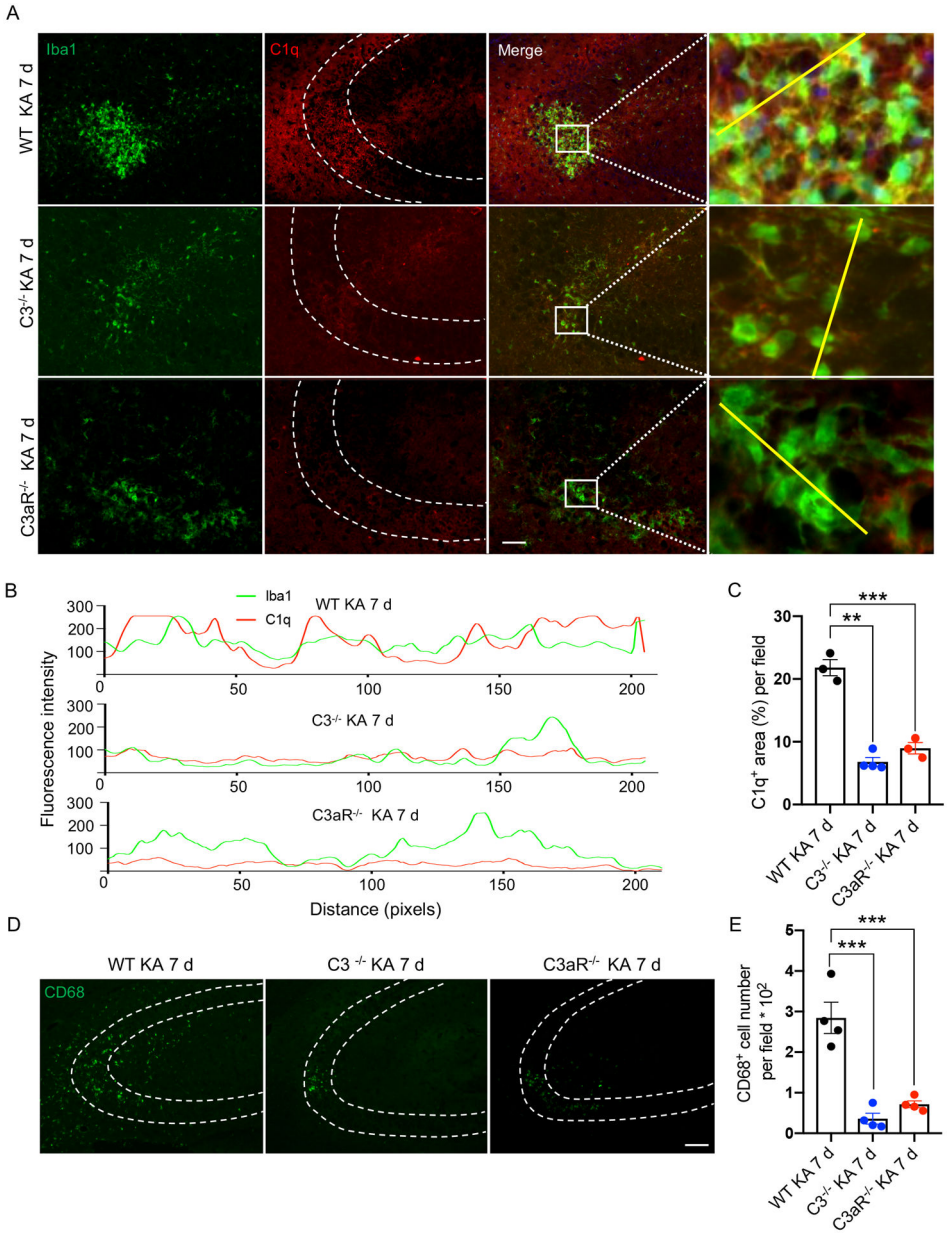

Fig. 5: Status epilepticus-triggered activation of microglia is reduced by complement C3 and C3aR deficiency.

(A) Representative images showing activated microglia (Iba1^{+}/ C1q^{+} cells) in the hippocampal CA3 region of WT, C3$^{-/-}$, and C3aR$^{-/-}$ mice, 7 d after status epilepticus induction. Scale bar: 50 μm. (B) Histograms illustrate fluorescence intensity of Iba1 or C1q channels along the yellow arrows in merged images of A. (C) Quantification of C1q^{+} cell density (WT n=3, C3$^{-/-}$ n=4, c3aR$^{-/-}$ n=3, 3 sections per mouse, ** p<0.01, *** p<0.001, one-way ANOVA). (D) Representative images show expression of CD68, a microglial activation marker, after status epilepticus induction in hippocampal CA3 region. Scale bar: 100 μm. (G) Quantification of CD68+ cell numbers (n=4 mice per group, 3 sections per mouse, *** p<0.001, one-way ANOVA).

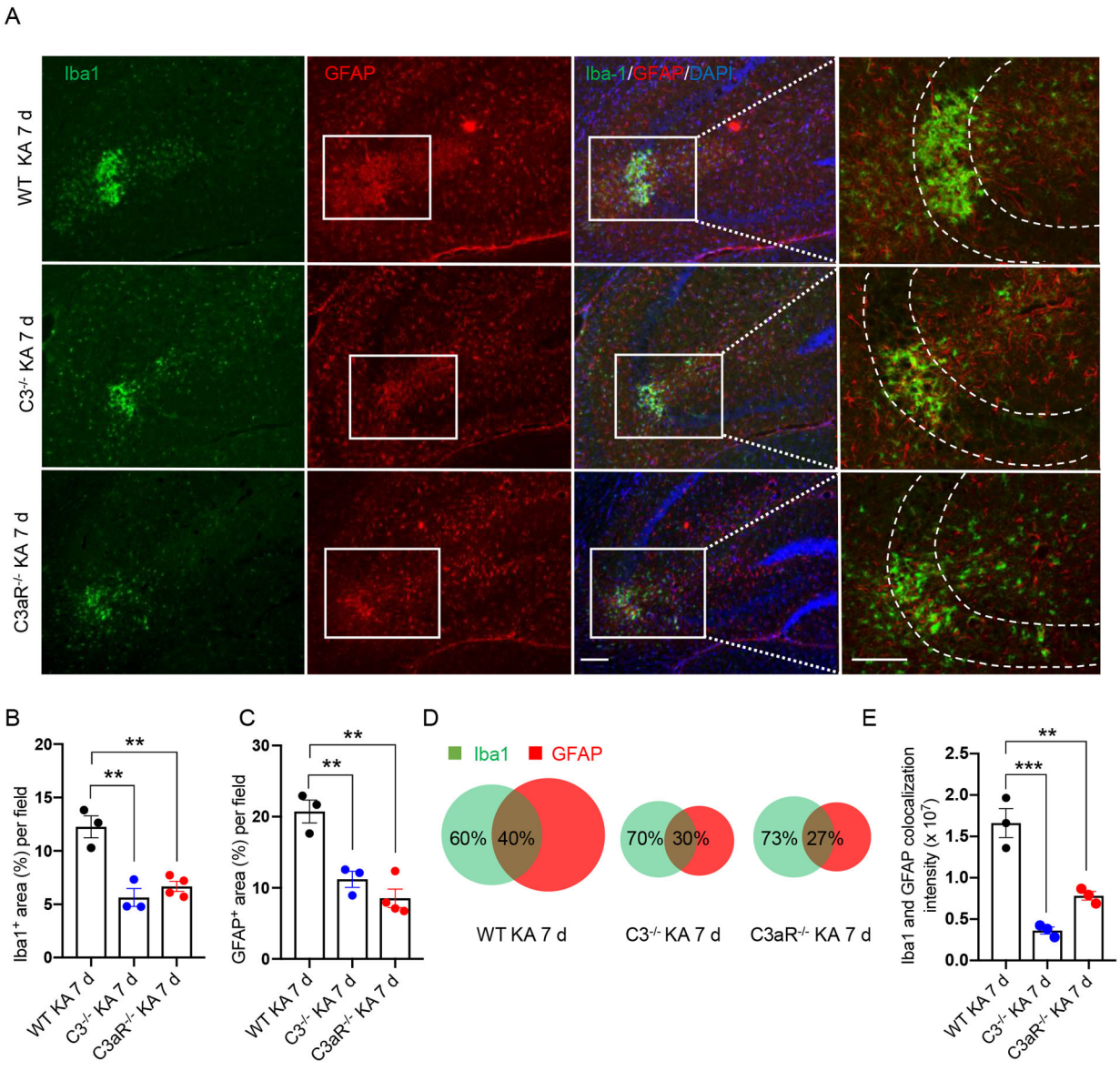

Fig. 6: Microglia-astrocyte interactions triggered by status epilepticus are downregulated in both complement C3 and C3aR KO mice.

(A) Representative images show Iba1$^+$ and GFAP$^+$ cells in the CA3 region of WT, C3$^{-/-}$, and C3aR$^{-/-}$ mice 7 d after status epilepticus induction. Scale bars: 100 μm. (B, C) Quantitative analysis of Iba1$^+$ and GFAP$^+$ cells after status epilepticus induction based on the hipp CA3 region (the last column of Fig. 5A). Astrogliosis reduction was obvious in both C3$^{-/-}$ and C3aR$^{-/-}$ mice at 7 d. (D, E) Quantitative analysis of Iba1/ GFAP co-localization (n=3 for WT and C3$^{-/-}$ groups, n=4 for C3aR$^{-/-}$ group, 3 sections per mouse, ** p<0.01, *** p<0.001, one-way ANOVA).

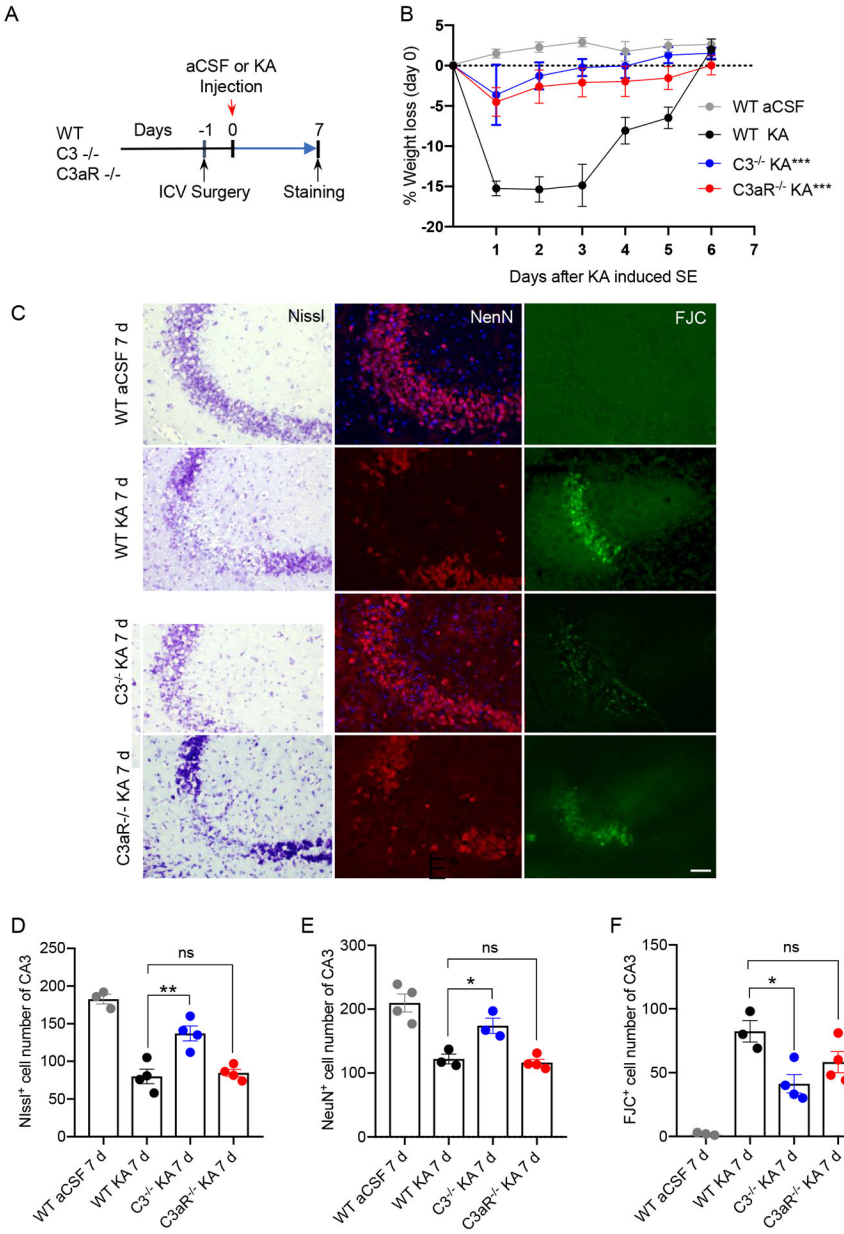

Fig. 7: Weight loss rate and neuroprotection in C3 KO mice after status epilepticus induction.

(A) Experimental time line. (B) C3 deficiency ameliorates mouse body weight loss following KA-induced status epilepticus (WT, n = 8; aCSF-injected, n = 7; KA-injected. $C3^{-/-}$ n=5 for KA, n=10 for $C3aR^{-/-}$, *** p<0.001, two-way ANOVA). (C) Representative images of CA3 region staining for Nissl, NeuN, and Fluoro Jade C, 7 d after status epilepticus induction. Scale bars: 50 μm. (D-F) Quantitative analysis of Nissl, NeuN, and FJC staining. Knock-out of C3 improved neuronal survival 7 d after status epilepticus induction. (n = 3–4 mice per group, ns = not significant, * p<0.05, ** p<0.01, one-way ANOVA).

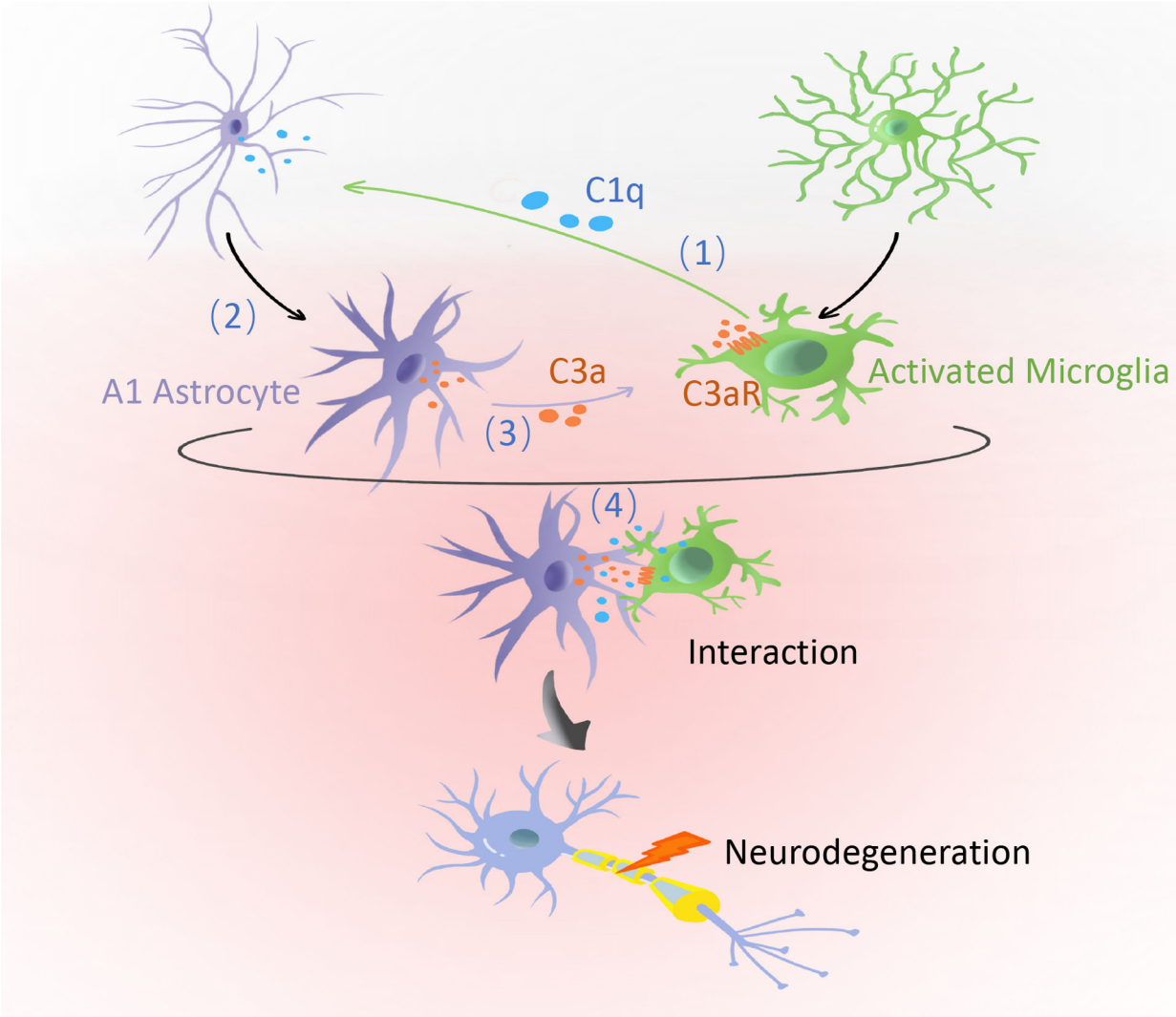

Fig. 8: Schematic diagram showing that C3-C3aR pathway mediates microglia-astrocyte interaction following status epilepticus.

In response to KA-induced seizures, the following processes might be triggered: (1) C1q expression is upregulated and released from activated microglia; (2) C1q from microglia induces A1 type, neurotoxic astrocyte activation and proliferation; (3) Complement C3 is upregulated and released by A1 astrocytes; (4) Microglia-astrocyte crosstalk mediated through C3-C3aR pathway leads to gliosis. Thus, seizure-induced microglia-astrocyte interaction and gliosis may cause neuronal injury.